

Effect of CNT radius on flattening contact behaviour of CNT-Al nanocomposite: A numerical approach

Rakesh Bhadra^{1,2}, Tamonash Jana^{1,3}, Anirban Mitra¹ and Prasanta Sahoo¹

¹Department of Mechanical Engineering, Jadavpur University, Kolkata 700032, India

²Department of Mechanical Engineering, Tezpur University, Sonitpur 784028, India

³Department of Mechanical Engineering, IEST, Shibpur 711103, India

Article Info

Article history:

Received June 24, 2023

Revised July 24, 2023

Accepted August 2, 2023

Keywords:

Contact Simulation,
Flattening,
Nanotubes and Nanocomposites,
FEM.

ABSTRACT

In the present paper, a flattening contact analysis of CNT-Al nanocomposite is presented for both loading and unloading phases. APDL code is used in ANSYS framework to create the FE model to analyse the contact behaviour between a frictionless cylinder (CNT-Al) and a rigid flat. The developed model has been validated against established results of certain problems with lesser complexity. The contact force, contact area, von Mises stresses and nodal displacements are extracted from the simulated solution. These parameters are noted at the end of the loading step and also once unloading is completed from a certain interference. It has been found that as CNT radius increases, the contact properties get decreased. It's also observed that beyond a certain CNT radius, the contact properties of CNT-Al nanocomposite materials start to resemble those of the matrix material and eventually fall below the matrix material.

Copyright © 2023 Regional Association for Security and crisis management and European centre for operational research. All rights reserved.

Corresponding Author:

Anirban Mitra,
Department of Mechanical Engineering, Jadavpur University, Kolkata 700032, India.
Email: anirban.mitra@jadavpuruniversity.in

1. Introduction

Nanotechnology is one of the latest developments in the advancement of engineering and technological application. Continuous growth in nanocomposite applications in various domains establish its increasing importance and underscores its capabilities in enhancing material strength and capacity. In this regard, use of carbon nanotubes (CNTs) as reinforcement material in the nanocomposite, to obtain substantial improvements in material properties and its usefulness in arresting crack growth [Kirtania & Chakraborty, 2007], must be mentioned. A very interesting domain of application related to fluid mechanics has been recently brought forward, where, CNT embedded boundary layer is utilized for energy harvesting [He & Elazem, 2021]. The theory discussed in the paper relates to applications of nanosensors, thermal and nanocomposite materials, resonators, nanomechanical gears etc. In the field of solid mechanics, use of nanocomposites with embedded CNTs to mitigate problems related to contact is another area of application with potential. Contacting parts of machine elements (for example, gears, cams, bearings etc.), which are usually under rapid loading and unloading, are often susceptible to failure. At such contact interfaces there is asperity level contact resulting in high stresses being developed. Use of nanocomposites in such contact scenarios to improve the contact parameters is a possible solution and requires thorough research.

Loading and unloading contact analysis of cylinders/hemispheres with a rigid plate, that can be thought of as an imitation of a single asperity contact, is one of the foremost areas of research in the above-mentioned domain. Johnson (1985) developed an analytical model to understand the unloading contact behavior with a spherical indenter. The model's predictions were in-line with experimental observations reported by Tabor (1948). The analysis indicated that unloading perfectly followed an elastic path despite extremely high plastic

deformation. Indentation contact analyses have been taken up by a number of researchers over the years and analytical, as well as, numerical techniques have been applied to determine stress distribution and deliberate on the deformation mechanics of the system [Biwa & Störackers, 1995; Mesarovic & Fleck, 1999; Kucharski & Mröz, 2001; Taljat & Pharr, 2004; Kim et al, 2006]. In this regard it should be mentioned that finite element approach has become one of the most popular tools to analyse such problems due to advancement of computation capabilities of modern computers. One of the earlier finite-element based research work, carried out by Kral et. al (1993), discussed spherical rigid indentation contact of half sphere. Yan and Li (2003) conducted a finite element analysis of nonlinear nature dealing with spherical indentation. The above-mentioned research papers mainly concentrated on spherical indentation apart from Johnson (1985), who also proposed the first cylindrical elastic contact solution in terms of a closed form expression. Since then, there have been substantial number of research works conducted in the area of cylindrical contact and these models have been updated with inclusion of various complexities dealing with materials and contact conditions [Green, 2005; Sharma and Jackson, 2017; Xu et al, 2021; Jana et al, 2022].

Numerical models, especially finite element simulations, have also been utilized to study the characteristics and behaviour of CNT reinforced nanocomposites. Ahmed et al. (2020) developed a FEM numerical model using ANSYS simulation package considering large strain elastoplastic behaviour for determination of behaviours of CNTs in nanocomposite. Experimental and numerical analysis were utilized by Nouri et al. (2012) to determine the mechanical properties of a multi-walled carbon nanotube (MWCNT) fibre-reinforced Aluminium (Al) nanocomposite. Accurate prediction of the elastic modulus and hardness were obtained from the developed model. For the purpose of predicting impact of single-walled carbon nanotubes (SWCNT) volume % on reinforced Epoxy nanocomposite, Le & Huang (2015) performed two-dimensional nanoindentation simulations using FEM. It was discovered that increase in volume % of SWCNTs corresponded to a rise in hardness and elastic modulus of nanocomposites and it had an impact on contact behaviour. Dmitriev (2021) developed a numerical local contact model of a polymer-based nanocomposite in order to study mechanical behavior at the mesoscale level under dry sliding.

Fundamentally, there are two different types of contact problems, namely, indentation and flattening. The majority of research works mentioned in the above paragraph deal with indentation type of contact. According to the authors' best knowledge, literature on flattening contact analysis of CNT-Al nanocomposite on the basis of a finite element model is extremely rare, if not non-existent. The current simulation work is based on a 2-dimensional model and this 2D cylindrical model consists of a rigid flat along with an Al cylinder having embedded CNTs. Here, Al is the matrix material, while reinforcement is provided by the SWCNTs embedded in the matrix. The rigid flat has the purpose of flattening the nanocomposite in order to comprehend the influence of CNTs on the contact behaviour. There is a need for investigation of the effect of change in radius of CNTs in the contact behaviour of nanocomposites. The mesh convergence analysis has been carried out to verify the model for acceptance and obtain accurate results efficiently. The analysis is used to extracting the contact force, contact area, stress distribution and deformation behaviour, which may be helpful for creating a CNT reinforced nanocomposite for particular applications.

2. FE Model

For the present simulation study, a half-cylindrical CNT-Al nanocomposite (Al matrix reinforced with embedded SWCNTs) is taken to be under contact with a rigid flat. A finite element model is developed for carrying out the flattening analysis that consists of both the loading and unloading cycles. With the objective of reducing the computational burden on the available resources, a 2D quarter circular model is developed instead of a 3D cylindrical model. The present FE model is illustrated in Figure 1., which also shows the position of the CNTs inside the matrix. Center distance between the tubes is kept above three times the tube radius so that the effect of Van der Waals forces can be neglected. It should be mentioned here that the number of CNTs (which, of course, is a significant parameter in effecting contact behaviour) has been kept fixed. Also, only one type of distribution of the embedded CNTs has been considered for the present paper with a view to maintain brevity. The coordinate system for the model is selected in such a manner that the vertical axis of symmetry acts as the Y-axis, whereas, the horizontal base of the quarter-circle coincides with the X-axis. This model of 2D quarter-circular CNT-Al nanocomposite consists of two distinct segments. The first of which are the circular rings representing CNTs with CNT-specific properties, while, the remaining region of the quarter-circle represents the matrix and has the material properties of Al. Perfect bonding is assumed between the matrix material and the CNTs, ensuring that there is no slip or detachment [Kirtania & Chakraborty, 2007, 2018; Kaushik et al., 2022]. A straight line parallel to the horizontal base of the quarter-circle (i.e., the X-axis) is used to model the rigid flat (Figure 1.). Downward motion of the straight line produces the effect of loading, while the line is withdrawn to simulate the unloading phase.

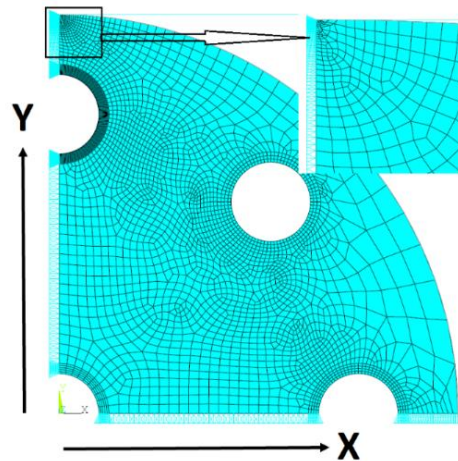


Figure 1. 2D finite element model of the SWCNT-Al nanocomposite and a enlarged view of the contact zone

It was previously mentioned that the purpose of the present investigation is to understand the nanocomposite contact behaviour in the context of variation of CNT radius. Hence, the number, distribution and the thickness of the tubes are kept constant, while, the radius of the CNTs is varied. The change in radius, of course, produces a change in the volume percentage of CNTs. Three different values of the radius are considered and these are 0.50, 0.60, and 0.70 nm, while the thickness of CNTs is fixed at 0.102 nm. It should be mentioned here that the radius of the cylinder is chosen as 4 nm. Supplied material properties for the nanotubes and the matrix are as follows [Ahmed et al., 2020; Nouri et al., 2012]:

- Elastic modulus for CNTs and Al are 1000 GPa and 70 GPa, respectively
- Poisson's ratio for CNTs and Al are 0.27 and 0.23, respectively

von Mises yield criteria and bilinear isotropic hardening model has been utilised to describe the inception of post-elastic regime and post-elastic behavior of the material. Frictionless contact is considered between the nanocomposite and rigid flat. Pure Lagrange multiplier contact algorithm is used in the analysis because it has the maximum accuracy and penetration is not required at the contact interface [Yan & Li, 2003; Jackson & Green, 2005]. The nanocomposite model is meshed with the PLANE183 element, a structural element having two degrees of freedom and the rigid flat is meshed using the TARGET169 element. The quarter circle's contacting curved surface has meshed with the CONTACT 172 element, which overlays the PLANE183 element and makes contact with the TARGET169 element.

The mesh for the current analysis is designed in such a way that it produces accurate enough results, yet, does not overburden the computational resources. The need for accuracy dictates that fine mesh is necessary in and around the contact zone and also in the neighborhood of the embedded nanotubes. But, away from the contact region, coarse meshing is sufficient. A detailed mesh convergence analysis is performed to decide upon the final configuration of the mesh. The mesh configuration used for the present analysis is shown in Figure 1. At this stage, a detailed description of the boundary conditions applied to the specific nodes of the model is warranted. The present analysis is quasi-static one with plane-stress condition and hence, the nodes coincident with the Y-axis are permitted vertical displacements only. On the other hand, as the asperity is connected with bulk, the nodes on the base (coincident with the X-axis) of the cylinder are completely restricted to move in any direction. Loading and unloading phases are simulated by moving the rigid flat towards the quarter circular nanocomposite in negative y-direction up to 0.60 nm and then withdrawing it up to its detachment from the cylindrical surface. Once the solution is completed, in the post-processing section of the FE analysis, contact force and area, stress distribution and nodal displacements are extracted.

3. Validation study

Validation of the present model is carried out before moving into extraction results for variation of tube radius. There are no similar studies in the existing literature, to which the present analysis of cylindrical nanocomposite flattening contact can be compared. But, the distinct aspects of the model can be separately validated. In one case, flattening of an isotropic, homogeneous material is considered [Ovcharenko et al., 2007], while in the other, indentation of CNT-Al nanocomposite by a Berkovic indenter is considered [Ahmed et al., 2020].

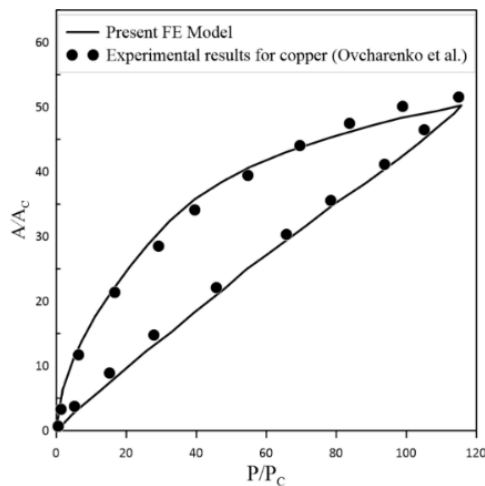


Figure 2. Comparison of generated normalised contact force vs. normalised contact area curve with results of Ovcharenko et al., (2007)

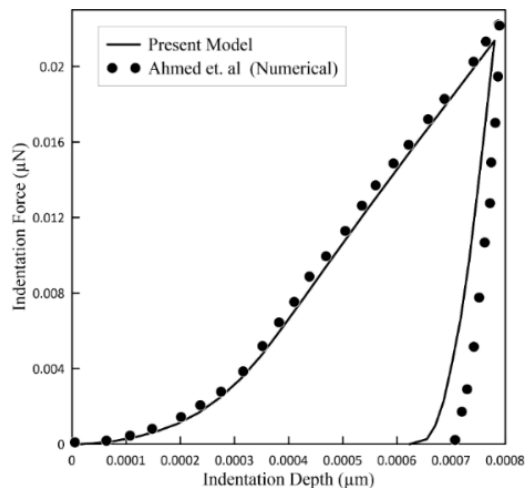


Figure 3. Comparison of generated indentation depth vs. indentation force curve with results of Ahmed et al. (2020)

The experimental results corresponding to loading and unloading of a 10 mm diameter copper sphere flattened by a sapphire-made flat [Ovcharenko et al., 2007] are compared with results obtained from the present simulation, where the CNT radius and thickness in the model are considered as zero. Figure 2. shows the comparative results of contact force vs. normalised contact area corresponding to Ovcharenko et al. [Ovcharenko et al., 2007] and the present model. Here, P and A stand for the contact pressure and contact area, respectively, while P_c and A_c represent critical contact pressure and area. Figure 3. depicts a comparison between contact force vs. indentation depth results (Berkovic indenter with an angle of 65.30 degrees with the vertical on a 10×10 nm CNT-Al nanocomposite) published by Ahmed et al. [Ahmed et al., 2020] and generated through the current simulation model. It is evident from both the comparisons that the outcomes produced by the current methodology exhibits a high degree of similarity, which serves to validate the model.

4. FE analysis

Contact stress distribution, displacements at the nodes (and corresponding deformation), contact area and contact force developed in the interface between CNT-Al nanocomposite and the rigid flat are significant output parameters (generated from the simulation model) that need to be studied. These different contact parameters can be extracted from the FE model on completion of the loading stage and at the end of unloading. The changes in these parameters are to be studied with respect to variation in the radius of the nanotubes, while the thickness and number of these tubes are kept constant.

Variation in contact force with increase (loading) and decrease (unloading) in interference is displayed in Figure 4 for flattening the nanocomposite while altering the radius of the CNTs (0.50 nm, 0.60 nm, and 0.70 nm). Furthermore, the contact force vs. interference plot for loading and unloading of pure aluminium is also provided in the same figure to act as a reference. The loading stage is continued till an interference of 0.60 nm and then the rigid flat withdrawn till detachment. The figure clearly illustrates that the increase in contact force with respect to interference is same up to a certain point, but once this point is passed, CNTs have a substantial role to play in the variation of contact force. The reason behind this behaviour is that at low interference there is not much deformation of the tubes and all the deformation is contained in the matrix.

An interesting phenomena is observed in contact force vs. interference diagram that the contact force decreases with respect to increase in radius of CNTs. Increase in radius increases the volume percentage and the natural expectation is that contact force to increase. However, the results shown in the figure are opposite in nature. The figure shows that during the flattening process contact force is lowest corresponding to the case of CNT radius 0.70 nm. In fact, it is even lower than the case of flattening of pure Al cylinder. This has happened due reduction of stiffness caused by increase in CNT radius. The phenomenon is supported by the results published and discussed by Ahmed et al. (2020). In an earlier published experimental work [Le & Huang, 2015], it was also reported that yield strength of nanocomposites decreased corresponding to higher volume % of CNT in the material.

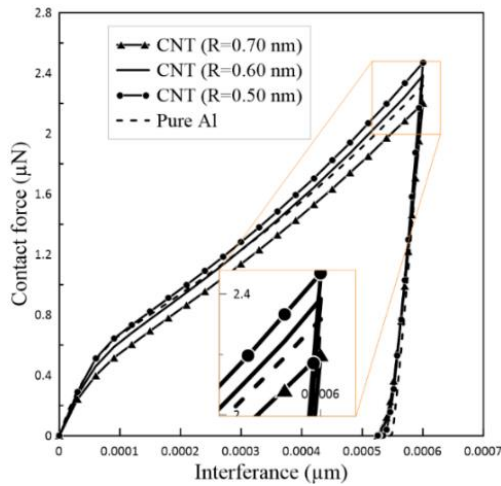


Figure 4. Variation of contact force against interference for different CNT radius

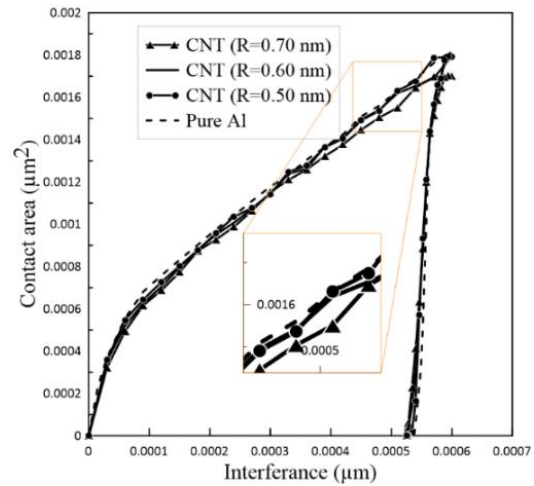


Figure 5. Variation of contact area against interference for different CNT radius

Figure 5. shows the contact area vs. interference plot for variation of CNT radius. This plot also consists of four curves representing the three different CNT radius (0.50 nm, 0.60 nm, and 0.70 nm) and one for pure Al. The contact area curves are close to each other in all variations of CNT radius, suggesting that the CNT radius has little impact on the contact area during flattening as well as the unloading phase. For lower interference, all of the curves overlap each other because of the reasons discussed in the contact force section.

4.1. Stress analysis

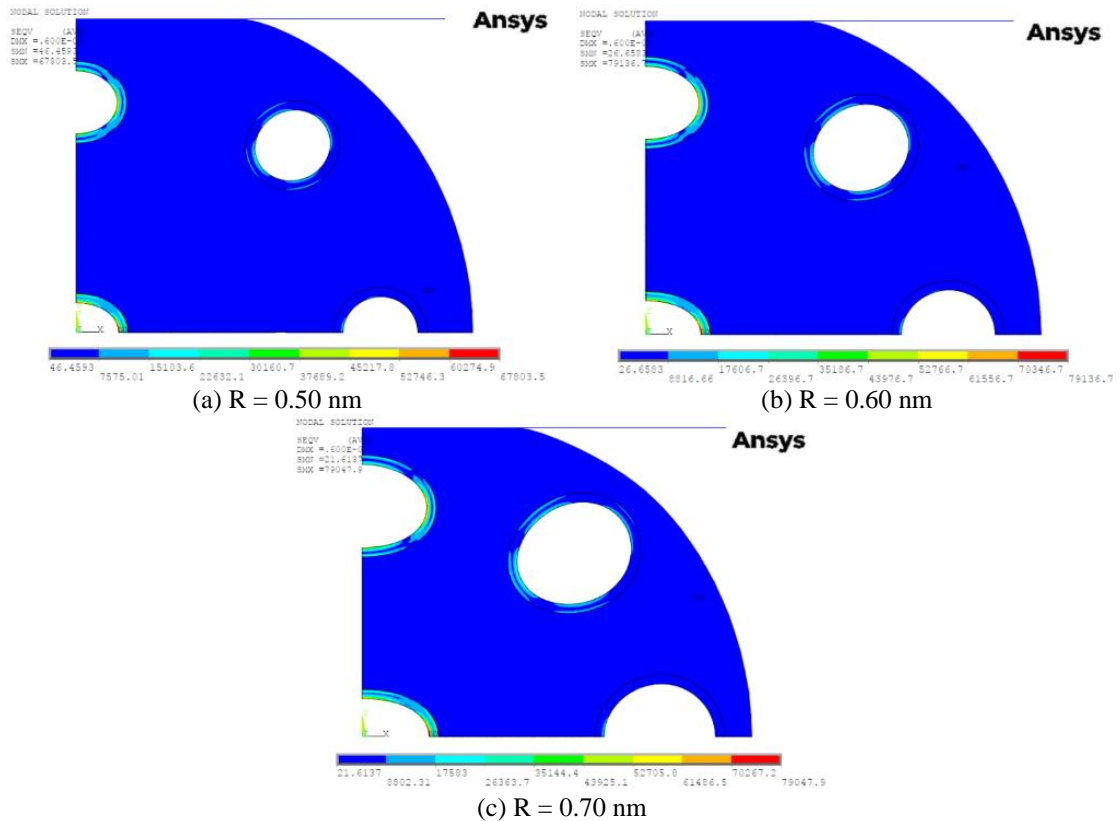


Figure 6. Average von-Mises stress distribution at an interference of 0.60 nm (Loading stage completed) with varying radius of CNTs.

An important component of contact analysis is comprehending the stress distribution over the nanocomposite on completion of loading as well as unloading step. At the end of loading, Figure 6 displays the contour plots of the average von Mises stress distribution, whereas Figure 7 displays the same at the end of

the unloading stage. In each of these two figures, the stress distribution plots are provided for three different CNT radius. The average von Mises stress is higher for nanotubes with a radius of 0.60 nm and lower for radius of 0.50 nm (see Figure 6). The figure also shows that the difference between the peak average von Mises stress developed for nanotube with radius of 0.60 nm and 0.70 nm is negligible. It is clearly visible from the figure that as the radius of the nanotube increases, there is reduction in stiffness (the thickness does not change) and there is higher deformation of the tube. So, the largest deformation occurs for the 0.7 nm radius nanotube situated closest to contact zone.

Another important aspect is to have an idea regarding how much von Mises stress is still present after all the load has been removed following the unloading step of flattening. Figure 7 shows the residual von Mises stress contour plots on completion of unloading (from an interference level of 0.60 nm). Higher plastic deformation of the material results in greater residual stress once unloading is completed. With increase of the radius of the CNTs, the peak residual von Mises stress increases, but resulting in similar stress distribution patterns.

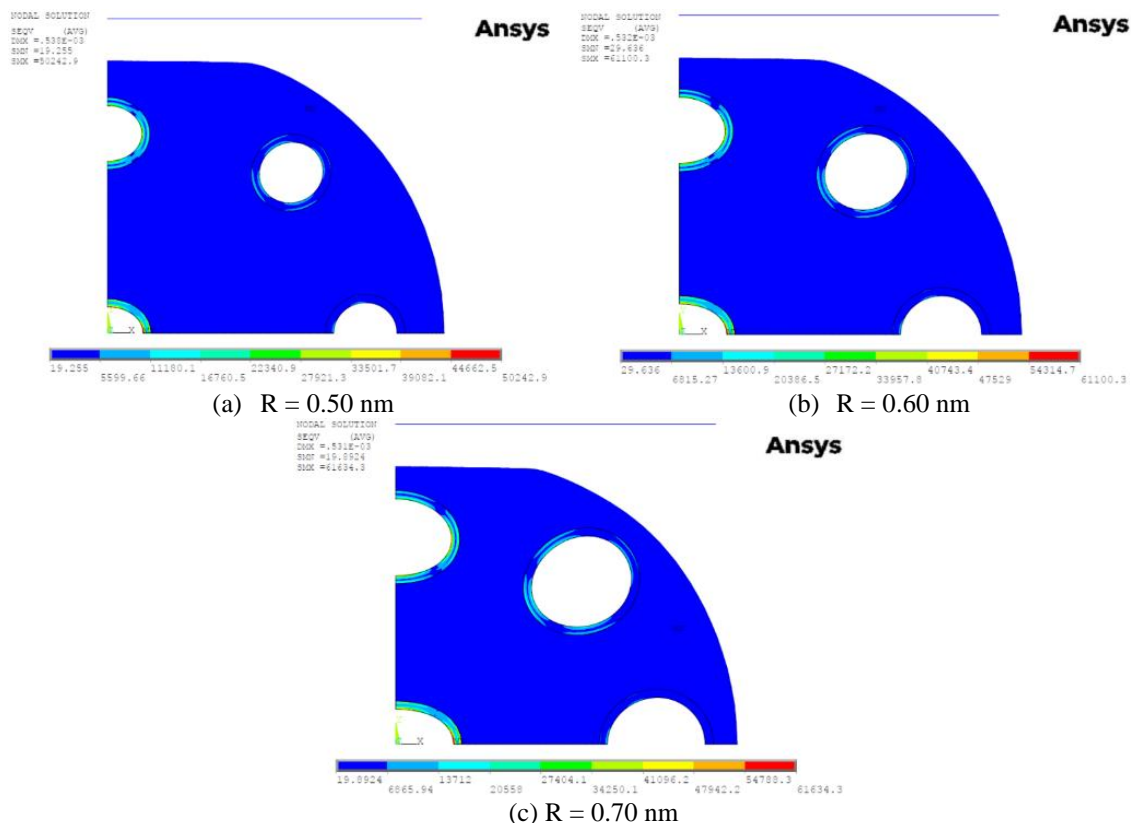


Figure 7. Residual von-Mises stress distribution at complete unloading (from an interference of 0.60 nm) with varying radius of CNTs.

4.2 Deformation analysis

In any flattening type contact analysis, study of deformation behaviour is an important aspect. Hence, analysis of deformation behaviour of CNT-Al nanocomposite during the loading phase and also in the unloading phase has been presented in this sub-section. The deformed geometry (corresponding to the nodes situated on the contacting cylindrical surface) after complete loading and unloading from an interference depth of 0.60 nm is presented in Figure 8. Three different radii of embedded CNT (0.50, 0.60 and 0.70 nm) are considered and plotted in the figure. Contour plots for y-directional deformation at the end of loading and unloading phases are furnished in Figures 9 and 10, respectively.

Figure 8 shows that during flattening the surface of the cylinder in contact with the rigid flat move downward together so that the nodes in contact at the loading stage are coincident with one another. Beyond the contact zone the displacement of the nodes is visible through the magnified view. It is seen that immediately after the contact zone there is negative x-direction displacement with respect to the undeformed state (shown by the blue curve in the figure). With increase in the x-coordinate, there is reduction in the negative displacement and beyond a certain point, positive x-direction displacements (which also increases

progressively) are obtained. The negative displacement of the nodes near the contact zone is greater for CNTs with higher radius and less so for CNTs with smaller radius. This occurs because CNTs with a larger radius result in less stiffness and correspond to greater deformation. For larger radius (with the same thickness) CNTs, as there is more deformation, it allows for the material to flow in that direction resulting in higher negative displacement. On the other hand, in case of CNTs with small radius, the tubes behave like rigid bodies and cause material compression at the interface between CNT and Al close to the contact zone. This compression of a part of the material just below the contact zone also results in a negative x directional displacement.

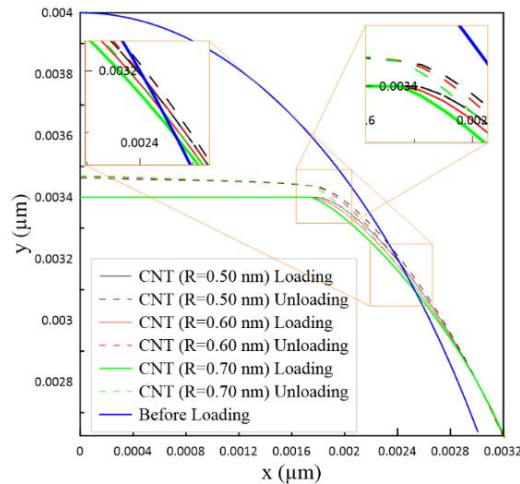


Figure 8. Deformed geometry of contact surface after complete loading and unloading from an interference depth of 0.60 nm with varying radius of CNTs. (R = 0.50, 0.60, and 0.70 nm).

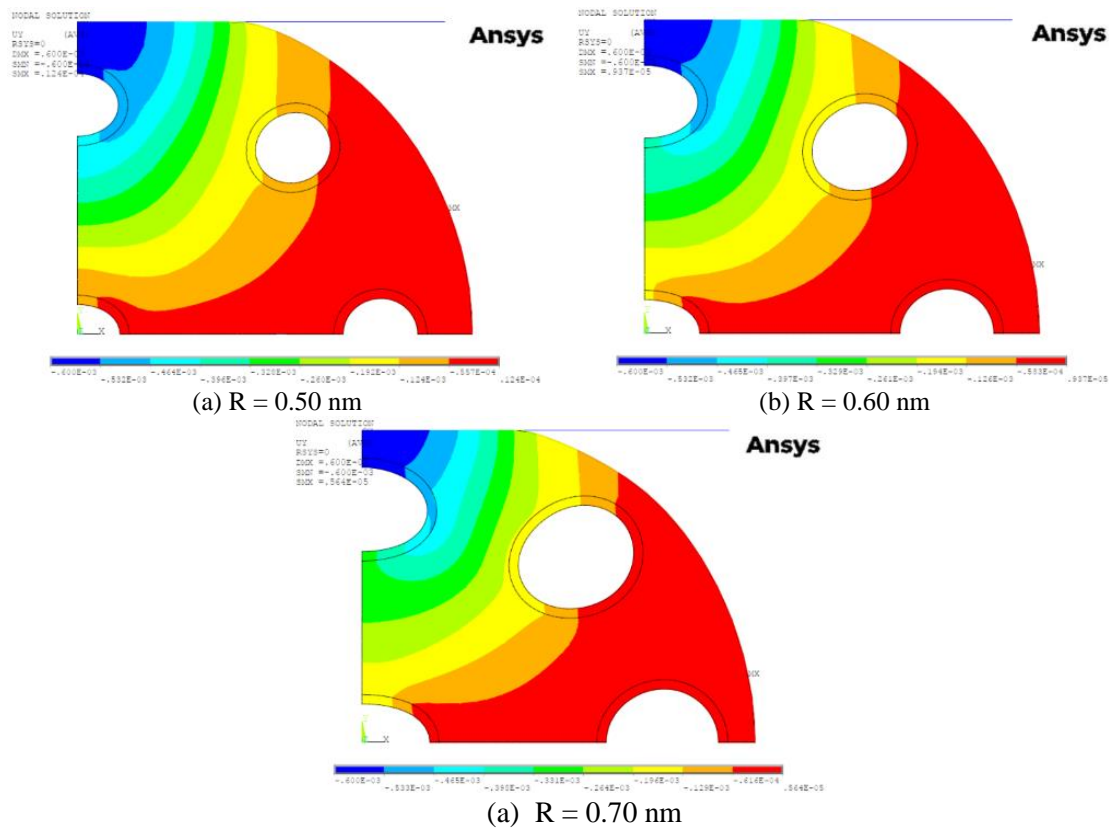


Figure 9. y-directional displacement contour plots at an interference of 0.60 nm.

Figures. 9 and 10 display the contour plots of nodal displacements in the y direction at the end of the loading and unloading stages of the flattening operation. Here, each figure is made up of three contour plots that show the variation in y-directional displacement for three distinct CNTs with radius of 0.5 nm, 0.6 nm, and 0.7 nm.

The contour plot in Figure 9 clearly shows that a higher area deforms for a lower radius at the end of loading stages, whereas lower area deforms for higher radius. Due to more deformation occurring in the larger radius CNT at the vicinity of the contact zone there is less load to be transferred to the matrix material. For lower radius CNT, higher amount of load transfer to the matrix material. Higher stiffness in lower radius results in a higher resistive force being applied to prevent deformation, which results in a higher amount of high deformation region observed near the contact zone.

The contour plot of nodal displacement at the completion of unloading is shown in Figure 10. At this stage, residual displacement exhibits similar patterns to those discussed in the loading stage.

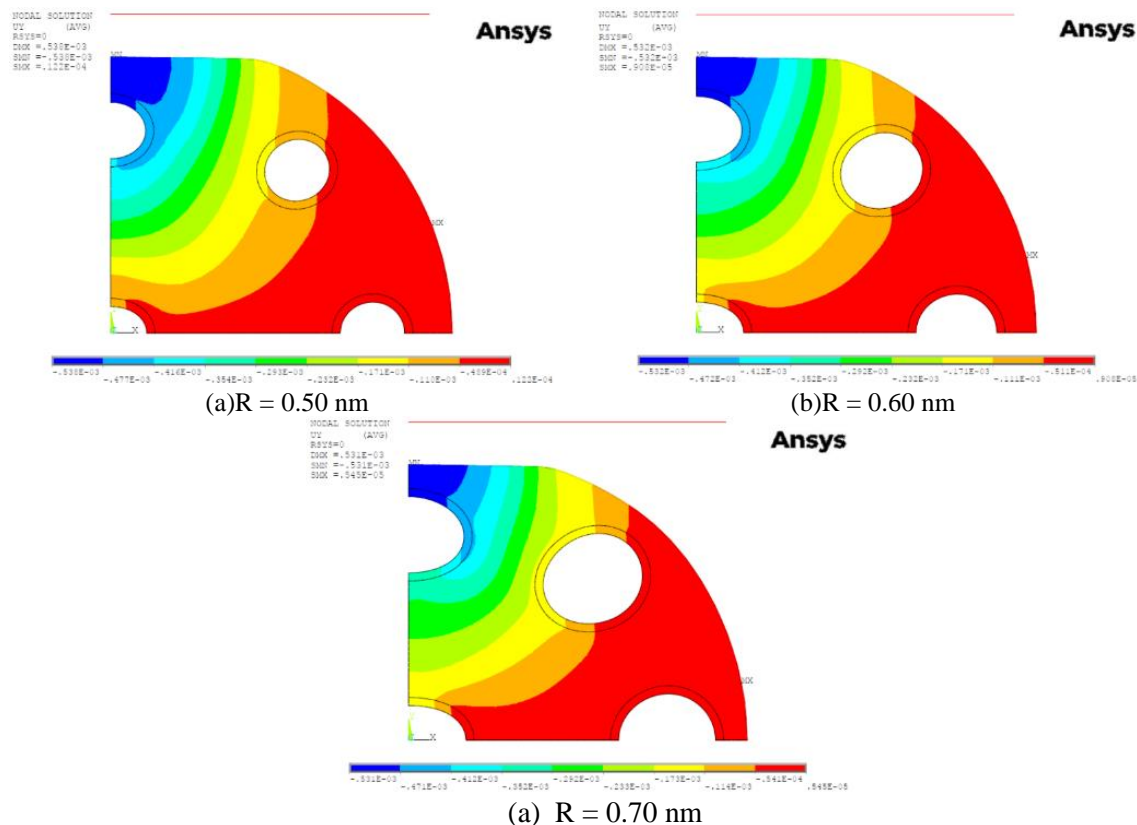


Figure. 10 y-directional displacement contour plots once unloading is completed from an interference of 0.60 nm.

5. Conclusions

Cylindrical flattening contact between SWCNT-Al nanocomposite and a rigid flat is investigated following a finite element-based model. The nanocomposite is flattened with a rigid flat till a certain interference level signifying the loading phase, while, withdrawal of the flat till complete detachment (from the previously mentioned interference) denotes the unloading phase of contact. The contact pair is appropriately meshed using different element types and a detailed convergence analysis is carried out to arrive at a proper mesh configuration. Validation of the developed model is achieved through comparisons against published data from literature. But it should be mentioned that the comparisons are with respect to similar contact scenarios, albeit with reduced complicity. An accurate FE model capable of prediction of contact behaviour of CNT-based nanocomposites under flattening is yet to be reported as per the authors' knowledge. In this respect the present simulation model has the ability to produce accurate results that can serve as benchmark results in the relevant domain. The primary objective of the present study is to investigate the changes observed in the different contact parameters due to variation of radius of the single-walled carbon nanotubes. Contact force as well as area, average developed average von Mises stresses, residual von Mises stresses and deformations are the

various contact parameters that have been considered in the present study. Observation of the generated results reveals the following points –

- There is decrease in contact force corresponding to a certain value of interference as the CNT radius increases. This might be due to reduction of stiffness as the larger radius tubes become more flexible. Additionally, it is seen that the contact force vs. interference plot for the 0.70 nm radius case is situated even lower than that of pure Al.
- The average von Mises stress increases with increase in radius of the CNTs in the nanocomposite. Similarly, the plastic deformation of the CNTs leads to the residual von Mises stresses to grow with increase in radius.
- The material away from the contact zone at the contact surface of the cylinder exhibits positive displacement as a result of material flow with an outward orientation, in contrast to the nodes near the contact zone of the cylinder contact surface, which are negatively displaced.
- When the radius is smaller, more material is observed to be affected and displaced in the loading direction as well as more strongly affected zones in close proximity to the contact zone.

References

- Ahmed, K., S., Ibrahim, I., & Keng, A. K. (2020). Advanced nanoindentation simulations for carbon nanotube reinforced nanocomposites. *Heliyon*, 6(8), e04575 (1-15).
- Biwa, S., & Störackers, B. (1995). An analysis of fully plastic Brinell indentation. *Journal of the Mechanics and Physics of Solids*, 8, 1303–1333.
- Dmitriev, A., I. (2021). Numerical Model of a Local Contact of a Polymer Nanocomposite and Its Experimental Validation. *Facta Universitatis, Series: Mechanical Engineering*, 19(1), 79-89.
- Green, I. (2005). Poisson ratio effects and critical values in spherical and cylindrical hertzian contacts. *International Journal of Applied Mechanics and Engineering*, 10(3), 451–462.
- He, J-H., & Elazem, N., Y., A. (2022). The Carbon Nanotube-Embedded Boundary Layer Theory for Energy Harvesting. *Facta Universitatis, Series: Mechanical Engineering*, 20(2), 211-235.
- Jackson, R., L., & Green, I. (2005). A finite element study of elasto-plastic hemispherical contact against a rigid flat. *J. Trib.*, 127(2), 343-354.
- Jana, T., Mitra, A., & Sahoo, P. (2022). Effect of yield strength on the static and dynamic behaviours of cylindrical contact: plane state of stress. *International Journal of Surface Engineering and Interdisciplinary Materials Science*, 10(1), 1-18.
- Johnson, K., L. (1985). *Contact Mechanics*. Cambridge University Press, Cambridge, MA.
- Kaushik, N., Sandeep, C., Jayaraman, P., Hillary, J., Srinivasan, V., P., Abisha Meji, M., & Barik, D. (2022). Finite Element Method-Based Spherical Indentation Analysis of Jute/Sisal/Banana-Polypropylene Fiber-Reinforced Composites. *Adsorption Science & Technology*, 2022, 1-19.
- Kim, S., H., Lee, B., W., Choi, Y., & Kwon, D., (2006). Quantitative determination of contact depth during spherical indentation of metallic materials - a FEM study. *Materials Science and Engineering: A*, 415, 59–65.
- Kirtania, S., & Chakraborty, D. (2007). Finite element based characterization of carbon nanotubes. *Journal of Reinforced Plastics and Composites*, 26(15), 1557-1570.
- Kirtania, S., & Chakraborty, D. (2018). Determination of thermoelastic properties of carbon nanotube/epoxy composites using finite element method. *Journal of Materials Engineering and Performance*, 27, 3783-3788.
- Kral, E. R., Komvopoulos, K., & Bogy, D., B. (1993). Elastic-plastic finite element analysis of repeated indentation of a half-space by a rigid sphere.
- Kucharski, S., & Mröz, Z. (2001). Identification of plastic hardening parameters of metals from spherical indentation tests. *Materials Science and Engineering: A*, 318, 65–76.
- Le, M. T., & Huang, S. C. (2015). Mechanical characterization of carbon nanotube-reinforced polymer nanocomposite by nanoindentation using finite element method. *Sensors and Materials*, 27(8), 617-624.
- Mesarovic, D., J., & Fleck, N., A. (1999). Spherical indentation of elastic–plastic solids. *Proceedings of the Royal Society of London. Series A*, 455, 2707–2728.

- Nouri, N., Ziaei-Rad, S., Adibi, S., & Karimzadeh, F. (2012). Fabrication and mechanical property prediction of carbon nanotube reinforced Aluminum nanocomposites. *Materials & Design*, 34, 1-14.
- Ovcharenko, A., Halperin, G., Verberne, G., & Etsion, I. (2007). In situ investigation of the contact area in elastic-plastic spherical contact during loading-unloading. *Tribology Letters*, 25(2), 153-160.
- Sharma, A., & Jackson, R. L. (2017). A Finite Element Study of an Elasto-Plastic Disk or Cylindrical Contact Against a Rigid Flat in Plane Stress with Bilinear Hardening. *Tribology Letters*, 65(3), 112 (1-12).
- Tabor, D. (1948). A simple theory of static and dynamic hardness. *Proceedings of the Royal Society of London. Series A*, 192, 247-274.
- Taljat, B., & Pharr, G.M. (2004). Development of pile-up during spherical indentation of elastic-plastic solids. *International Journal of Solids and Structures*, 41, 3891-3904.
- Xu, K., Chu, N., R., & Jackson, R., L. (2022). An investigation of the elastic cylindrical line contact equations for plane strain and stress considering friction. *Proceedings of the Institution of Mechanical Engineers, Part J: Journal of Engineering Tribology*, 236(9) 1889-1897.
- Yan, S., L., & Li, L., Y. (2003). Finite element analysis of cyclic indentation of an elastic-perfectly plastic half-space by a rigid sphere. *Proceedings of the Institution of Mechanical Engineers, Part C: Journal of Mechanical Engineering Science*, 217(5), 505-514.